



Cite this: *Chem. Commun.*, 2025, 61, 9420

Received 30th April 2025,  
Accepted 21st May 2025

DOI: 10.1039/d5cc02428e

rsc.li/chemcomm

# Unexpected cyclization of $\beta$ -(hydroxymethyl)-phosphole into 1-phospha-1,6a-dihydrophosphapentalene: a fused 1,3-butadiene-based luminophore†

Tomohiro Higashino,<sup>a</sup> Riku Minobe,<sup>a</sup> Tomoya Machino<sup>a</sup> and Hiroshi Imahori<sup>a,b,c</sup>

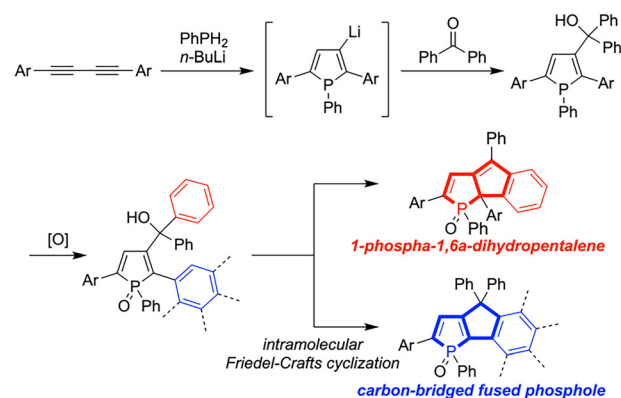
**During the planned synthesis of carbon-bridged fused phospholes, an unexpected intramolecular cyclization of  $\beta$ -(hydroxymethyl)-phosphole yielded 1-phospha-1,6a-dihydrophosphapentalene, besides the expected cyclized product. The solid-state emission of 1-phospha-1,6a-dihydrophosphapentalene indicates its potential as a 1,3-butadiene-based solid-state luminophore.**

Incorporating bridging structures into  $\pi$ -systems can modulate their optical and electronic properties by introducing structural constraints and electronic perturbations *via* heteroatoms. Phosphorus-bridged  $\pi$ -conjugated molecules, especially fused phosphole derivatives, exhibit remarkable physicochemical properties, such as highly electron-accepting ability and intense emission with high fluorescence quantum yields.<sup>1–9</sup> In addition, carbon-bridged structures offer optimal conjugation due to their highly planar and rigid conformation.<sup>10–15</sup> In this context, a rational synthetic methodology for carbon-bridged fused phospholes would be useful toward effectively  $\pi$ -extended phosphole-based functional materials.

Although  $\beta$ -(hydroxymethyl)phospholes serve as key precursors to carbon-bridged fused phospholes, successful synthetic protocols for  $\beta$ -substituted 2,5-diarylphospholes remain limited.<sup>16,17</sup> Given the proposed reaction mechanism for the *n*-BuLi mediated synthesis of 2,5-diarylphospholes from 1,3-butadiynes and phenylphosphine (PhPH<sub>2</sub>), we envisioned that treating 1,3-butadiynes with

a stoichiometric amount of *n*-BuLi could generate  $\beta$ -lithiated intermediates.<sup>16–18</sup> Subsequent reaction with ketones and oxidation of phosphorus atom would yield  $\beta$ -(hydroxymethyl)phosphole *P*-oxides, which could be transformed into carbon-bridged fused phosphole *P*-oxides *via* intramolecular Friedel–Crafts cyclization. Following this strategy, we pursued the straightforward synthesis of carbon-bridged fused phospholes and unexpectedly discovered the formation of 1-phospha-1,6a-dihydrophosphapentalene (Scheme 1). Though Latscha and co-workers reported the synthesis of a 1-phospha-1,6a-dihydrophosphapentalene derivative in 1991,<sup>19</sup> further exploration and detailed analysis of their properties have not been conducted. Herein, we report the intramolecular Friedel–Crafts cyclization reaction of  $\beta$ -(hydroxymethyl)phospholes, yielding 1-phospha-1,6a-dihydrophosphapentalene as well as anticipated carbon-bridged fused phospholes.

First, we embarked on synthesizing  $\beta$ -substituted 2,5-diarylphospholes (Scheme 2). Treating PhPH<sub>2</sub> with a stoichiometric amount of *n*-BuLi (1 equiv.) and subsequently adding 1,4-diphenylbutadiyne generated the  $\beta$ -lithiated phosphole intermediate at –78 °C. Reacting this intermediate with benzophenone at



**Scheme 1** *n*-BuLi mediated synthesis of  $\beta$ -substituted phospholes and intramolecular Friedel–Crafts cyclization of  $\beta$ -(hydroxymethyl)phospholes.

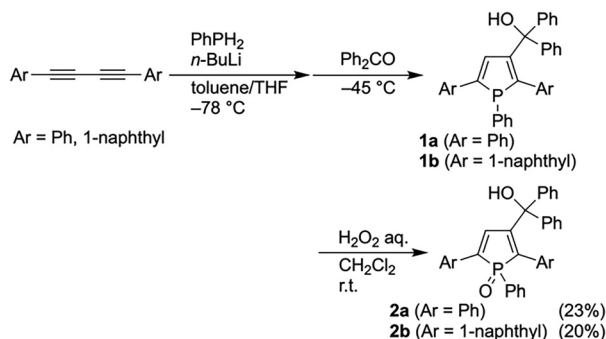
<sup>a</sup> Department of Molecular Engineering, Graduate School of Engineering, Kyoto University, Kyoto, 615-8510, Japan. E-mail: t-higa@scl.kyoto-u.ac.jp, imahori@scl.kyoto-u.ac.jp

<sup>b</sup> Institute for Integrated Cell-Material Sciences (iCeMS), Kyoto University, Kyoto, 606-8501, Japan

<sup>c</sup> Institute for Liberal Arts and Sciences (ILAS), Kyoto University, Kyoto, 606-8316, Japan

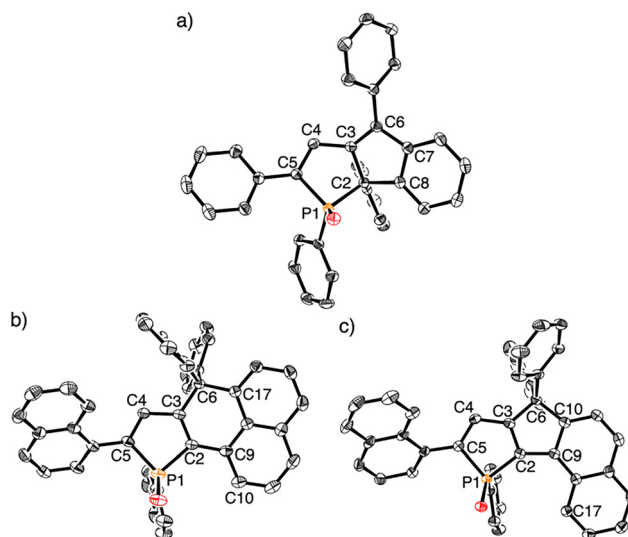
† Electronic supplementary information (ESI) available: Experimental section, synthetic details, X-ray crystallographic details, computational investigation into reaction mechanism, optical properties, HR-MS, and NMR spectra. CCDC 2424364 (3), 2424363 (4), and 2424362 (5). For ESI and crystallographic data in CIF or other electronic format see DOI: <https://doi.org/10.1039/d5cc02428e>



Scheme 2 Synthesis of  $\beta$ -(hydroxymethyl)phospholes **1** and **2**.

–45 °C then afforded the desired  $\beta$ -(hydroxymethyl)phosphole **1a**. Due to the instability of the  $\sigma^3, \lambda^3$ -phosphole **1a** under ambient conditions, it was difficult to isolate using conventional silica-gel column chromatography. Therefore, the crude **1a** was converted into the stable phosphole oxide **2a** by oxidation with an aqueous  $\text{H}_2\text{O}_2$  solution. Additionally, we synthesized the  $\beta$ -substituted phospholes **1b** and **2b** in a similar manner using 1,4-di(1-naphthyl)butadiyne.

Next, we conducted the intramolecular Friedel–Crafts cyclization reaction of phosphole *P*-oxides **2** in the presence of  $\text{BF}_3 \cdot \text{Et}_2\text{O}$  as reported by Yamaguchi and co-workers (Scheme 3).<sup>20–23</sup> When **2a** was treated with 1 equivalent of  $\text{BF}_3 \cdot \text{Et}_2\text{O}$ , it was completely recovered after conventional aqueous workup, suggesting that the stoichiometric amount of  $\text{BF}_3$  was consumed to form a phosphine oxide- $\text{BF}_3$  adduct.<sup>24,25</sup> Conversely, treating **2a** with an excess amount of  $\text{BF}_3 \cdot \text{Et}_2\text{O}$  (5 equiv.) proceeded smoothly, yielding a new product **3** in high yield (87%). Surprisingly, the crystal structure of **3** unambiguously revealed a 1-phospha-1,6a-dihydropentalene skeleton, not the anticipated carbon-bridged fused phosphole (Fig. 1a and Table S1, ESI†). Notably, the two phenyl groups at the 1- and 6a-positions adopted a *syn*-configuration, and the *anti*-isomer was not obtained. The selective formation of the *syn*-isomer can be explained by the steric hindrance of the phenyl group on the phosphorus atom in the

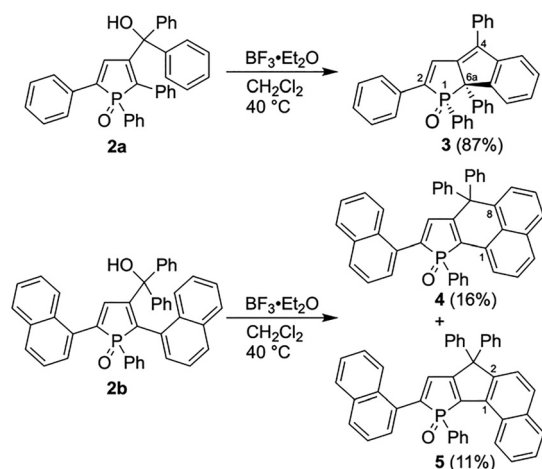
Fig. 1 X-Ray crystal structures of (a) **3**, (b) **4**, and (c) **5**. Thermal ellipsoids represent 50% probability. Hydrogen atoms and solvent molecules are omitted for clarity.

transition state (*vide infra*). The C–C bond lengths of C2–C3 (1.5260(18) Å) and C2–C8 (1.5218(18) Å) clearly indicate that **3** possesses an  $\text{sp}^3$ -carbon atom at the 6a-position (C2 atom in Fig. 1a). The C4–C5 (1.3584(18) Å) and C3–C6 (1.3553(18) Å) bond lengths are almost comparable to a typical C=C double bond length (1.35 Å) in 1,3-butadiene.<sup>26</sup> Thus, the crystal structure clearly corroborates that **3** possesses a 1,3-butadiene skeleton.

In contrast to the reaction of **2a**, the reaction of **2b** with  $\text{BF}_3 \cdot \text{Et}_2\text{O}$  resulted in two new compounds, **4** (16%) and **5** (11%), which were successfully separated by HPLC–GPC (Scheme 3). The structures of **4** and **5** were confirmed by single crystal X-ray diffraction analysis, revealing them to be the expected carbon-bridged 1,8- and 1,2-fused phospholes, respectively (Fig. 1b, c and Table S1, ESI†). The slightly higher yield of **4** compared to **5** is attributed to the higher reactivity at the  $\alpha$ -position than the  $\beta$ -position of naphthalene.

To elucidate the reaction mechanism of the intramolecular Friedel–Crafts cyclization reactions and understand the selectivity of the products, we conducted the density functional theory (DFT) calculations at the  $\omega\text{B97XD}/6\text{-}311\text{G}++(\text{d,p})/\text{B3LYP}/6\text{-}31+\text{G}(\text{d,p})$  level with the polarizable continuum model (PCM) using  $\text{CH}_2\text{Cl}_2$  as a solvent (Tables S2 and S3, ESI†). Given that one equivalent of  $\text{BF}_3$  is consumed to form the phosphine oxide- $\text{BF}_3$  adduct (*vide supra*), we set the phosphine oxide- $\text{BF}_3$  adducts **S1** and **S2** as starting materials for the intramolecular cyclization.

First, we examined the reaction mechanism for 2,5-diphenylphosphole **S1** (Fig. 2). The hydroxy group of **S1** is activated by additional  $\text{BF}_3$ , generating the cation intermediate **INT1** via **TS1**. Intramolecular C–C bond formation then occurs via **TS2a–c**, and the deprotonation of the resultant intermediates **INT2a–c** affords the products. The energy barrier for **TS2a** ( $\Delta G^\ddagger = +17.9 \text{ kcal mol}^{-1}$ ) to produce a 1-phospha-1,6a-dihydropentalene with *syn*-configuration **P1a** is smaller than those for **TS2b** ( $\Delta G^\ddagger = +20.2 \text{ kcal mol}^{-1}$ ) and **TS2c** ( $\Delta G^\ddagger = +20.6 \text{ kcal mol}^{-1}$ ), which yield

Scheme 3 Intramolecular cyclization reaction of phosphole *P*-oxides **2** in the presence of  $\text{BF}_3 \cdot \text{Et}_2\text{O}$ .

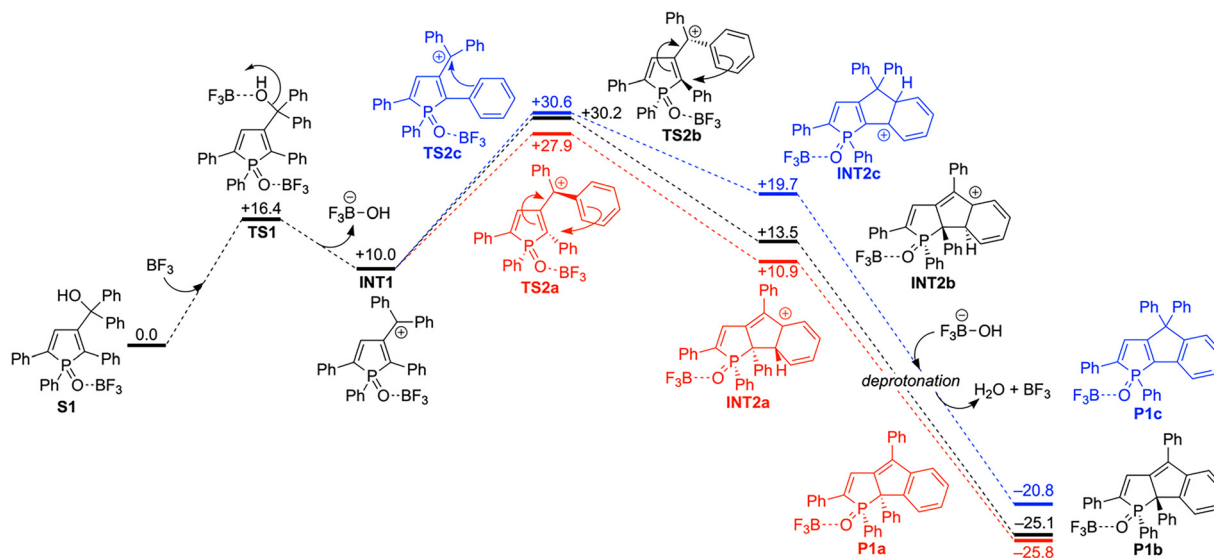


Fig. 2 Mechanistic studies of intramolecular cyclization for 2,5-diphenylphosphole **S1** using DFT methods at the  $\omega$ B97XD/6-311G++(d,p)//B3LYP/6-31+G(d,p) level with polarizable continuum model (PCM) using  $\text{CH}_2\text{Cl}_2$  as the solvent. The relative Gibbs free energy values are given in  $\text{kcal mol}^{-1}$  units.

a 1-phospha-1,6a-dihydropentalene with *anti*-configuration **P1b** and a carbon-bridged fused phosphole **P1c**, respectively. In **TS2a**, the C3–C6 bond length (1.406 Å) is significantly shorter than the non-conjugated  $\text{C}(\text{sp}^2)\text{--C}(\text{sp}^2)$  single bond length (1.48 Å),<sup>27</sup> implying the contribution of a  $\text{C}=\text{C}$  double bond (Fig. S1, ESI†). The small torsion angle of C2–C3–C6–C7 (19°) is consistent with the double bond character of the C3–C6 bond. **TS2a** thus possesses an allylic cation-like structure. Furthermore, the short H8...F1 distance in **TS2a** (2.13 Å) implies activation of the C8 atom by the  $\text{CH}\cdots\text{F}$  hydrogen bond interaction (2.20–2.26 Å).<sup>28</sup> Although the structural features of **TS2b** (C2–C3: 1.459 Å; C3–C6: 1.404 Å;  $\angle$  C2–C3–C6–C7: 18°) also suggest an allylic cation-like structure, the larger torsion angle of C2–P1–O1–B1 for **TS2b** (73°) compared to **TS2a** (58°) suggests significant steric repulsion between the  $\text{BF}_3$  moiety and the phenyl ring at the 2-position, destabilizing **TS2b**.

In contrast to **TS2a** and **TS2b**, the long C3–C6 bond length (1.497 Å) and the large torsion angle of C2–C3–C6–C8 (81°) agree with the single bond character of the C3–C6 bond. As a result, the localized positive charge on the C6 atom destabilizes **TS2c**. Overall, **TS2a** is stabilized by the delocalized positive charge over the allylic cation-like structure, minimal unfavorable steric repulsion, and activation through intramolecular  $\text{CH}\cdots\text{F}$  hydrogen bond interaction. Since the C–C bond formation should be the rate-determining step, the smallest  $\Delta G^\ddagger$  value of **TS2a** clearly supports the selective formation of 1-phospha-1,6a-dihydropentalene with *syn*-configuration.

The calculated reaction mechanism for 2,5-dinaphthylphosphole **S2** is depicted in Fig. S2 (ESI†). We examined three pathways from the cation intermediate **INT3** to form the possible products, the 1-phospha-1,6a-dihydropentalene **P2a** and two carbon-bridged fused phospholes **P2b** and **P2c**. In contrast to **S1**, the  $\Delta G^\ddagger$  value of **TS4a** for forming a 1-phospha-1,6a-dihydropentalene **P2a** ( $\Delta G^\ddagger = +22.0 \text{ kcal mol}^{-1}$ ) is considerably higher than those of **TS4b** ( $\Delta G^\ddagger = +16.5 \text{ kcal mol}^{-1}$ ) and **TS4c** ( $\Delta G^\ddagger = +17.0 \text{ kcal mol}^{-1}$ ) for carbon-bridged fused phospholes **P2b** and

**P2c**. The steric hindrance of the naphthyl group at the 2-position against the diphenylmethyl group at the 3-position destabilizes **TS4a** (Fig. S3 and S4, ESI†). Moreover, the higher reactivity of the naphthyl group compared to the phenyl group toward electrophilic substitution reactions promotes the formation of carbon-bridged fused phospholes. Therefore, the selectivity of the products can be rationalized by the steric hindrance and reactivity of the aryl substituents at the 2-position on the phosphole skeleton. Additionally, the slightly smaller  $\Delta G^\ddagger$  value of **TS4b** compared to **TS4c** is attributed to the higher reactivity at the  $\alpha$ -position than the  $\beta$ -position of naphthalene, which aligns with the higher yield of 1,8-fused phosphole **4** compared to 1,2-fused phosphole **5** (*vide supra*).

We examined the optical properties of the products **3–5** (Fig. 3 and Table S4, ESI†). The blue-shifted absorption and fluorescence of **3** compared to the reference phosphole **6** can be attributed to the less effective interaction of  $\sigma^*$ -orbital of the P–C bond and  $\pi^*$ -orbital of the butadiene moiety in **3** because of the  $\text{sp}^3$  carbon atom neighboring the phosphorus atom. In addition, the *s-trans* configuration of the 1,3-butadiene skeleton in **3** may also contribute to the blue-shifted absorption.<sup>29</sup> On the other hand, the carbon-bridged fused phospholes **4** and **5** exhibit red-shifted absorption and fluorescence in comparison with the non-fused phosphole **7**. The  $\text{sp}^3$  carbon atom contributes to the effective  $\pi$ -extension resulting from the co-planarization of the naphthyl group.

Notably, 1-phospha-1,6a-dihydropentalene **3** exhibits distinct fluorescence even in the solid state whereas phosphole derivatives **4–7** show no emission in the solid state (Fig. S5, ESI†). Importantly, the  $\Phi_F$  value of **3** in the solid state (0.25) is considerably higher than that in solution (0.04). Given that aryl-substituted 1,3-butadiene structure have emerged as effective scaffolds for solid-state emission owing to their aggregation-induced emission (AIE) features,<sup>30–34</sup> a 1-phospha-1,6a-dihydropentalene structure can also be a promising platform for fused 1,3-butadiene-based solid-state fluorophores.



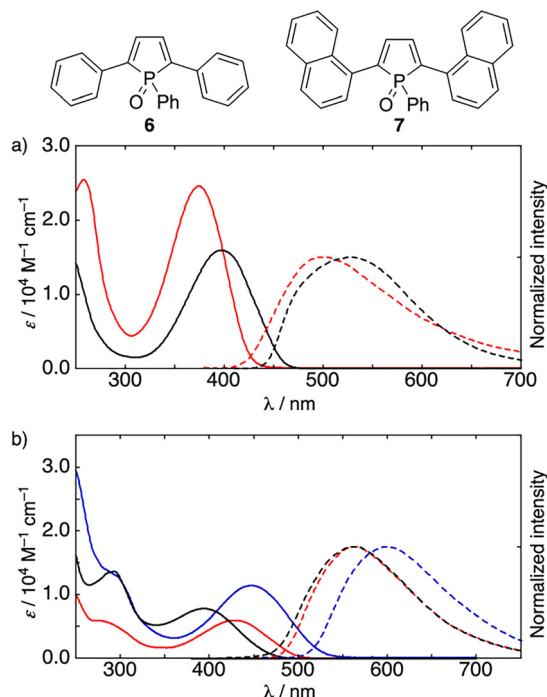


**Fig. 3** UV/Vis absorption (solid lines) and normalized fluorescence (dashed lines) spectra of (a) **3** (red) and **6** (black), and (b) **4** (red), **5** (blue), and **7** (black) in  $\text{CH}_2\text{Cl}_2$ . For fluorescence measurements, the samples were excited at  $\lambda_{\text{ex}} = 370$  nm for **3**,  $\lambda_{\text{ex}} = 430$  nm for **4**,  $\lambda_{\text{ex}} = 450$  nm for **5**, and  $\lambda_{\text{ex}} = 395$  nm for **6** and **7**.

In summary, we pursued a rational synthetic protocol for carbon-bridged fused phospholes and unexpectedly discovered an intramolecular cyclization reaction of  $\beta$ -(hydroxymethyl)-phosphole **2a**, resulting in the formation of 1-phospha-1,6a-dihydropentalene **3**. Theoretical investigations into the reaction mechanism described plausible pathways, suggesting that the product selectivity is governed by the substituents at the 2-position on the phosphole skeleton. Importantly, we revealed the solid-state emissive nature of **3** for the first time, indicating its potential as a 1,3-butadiene-based solid-state luminophore. Thus, we believe that further investigation on the intramolecular cyclization reaction of  $\beta$ -(hydroxymethyl)phospholes will pave the way for developing 1-phospha-1,6a-dihydropentalenes and carbon-bridged fused phospholes as promising organic functional materials.

This work was supported by the JSPS (KAKENHI Grant Numbers JP20H05841, JP22K05066, and JP25K01874 (T. H.), JP20H05832 and JP23H00309 (H. I.)).

## Data availability

Data supporting this article is included in the ESI.† Crystallographic data have been deposited at the CCDC with deposition numbers 2424364 (**3**), 2424363 (**4**), and 2424362 (**5**).

## Conflicts of interest

There are no conflicts to declare.

## Notes and references

- 1 Y. Matano and H. Imahori, *Org. Biomol. Chem.*, 2009, **7**, 1258–1271.
- 2 T. Baumgartner, *Acc. Chem. Res.*, 2014, **47**, 1613–1622.
- 3 D. Joly, P.-A. Bouit and M. Hissler, *J. Mater. Chem. C*, 2016, **4**, 3686–3698.
- 4 M. P. Duffy, W. Delaunay, P.-A. Bouit and M. Hissler, *Chem. Soc. Rev.*, 2016, **45**, 5296–5310.
- 5 P. Hibner-Kulicka, J. A. Joule, J. Skalik and P. Bałczewski, *RSC Adv.*, 2017, **7**, 9194–9236.
- 6 N. Asok, J. R. Gaffen and T. Baumgartner, *Acc. Chem. Res.*, 2023, **56**, 536–547.
- 7 T. Higashino, K. Ishida, T. Sakurai, S. Seki, T. Konishi, K. Kamada, K. Kamada and H. Imahori, *Chem. – Eur. J.*, 2019, **25**, 6425–6438.
- 8 K. Ishida, T. Higashino, Y. Wada, H. Kaji, A. Saeki and H. Imahori, *ChemPlusChem*, 2021, **86**, 130–136.
- 9 K. Zhang, X. Wang, Z. Zhou, J. Guo, H. Liu, Y. Zhai, Y. Yao, K. Yang and Z. Zeng, *Angew. Chem., Int. Ed.*, 2025, **64**, e202418520.
- 10 U. Scherf, *J. Mater. Chem.*, 1999, **9**, 1853–1864.
- 11 H. Tsuji and E. Nakamura, *Acc. Chem. Res.*, 2019, **52**, 2939–2949.
- 12 Y. Kurumisawa, T. Higashino, S. Nimura, Y. Tsuji, H. Iiyama and H. Imahori, *J. Am. Chem. Soc.*, 2019, **141**, 9910–9919.
- 13 Y. Zhang, T. Higashino, I. Nishimura and H. Imahori, *ACS Appl. Mater. Interfaces*, 2024, **16**, 67761–67770.
- 14 J. Wang and X. Zhan, *Acc. Chem. Res.*, 2021, **54**, 132–143.
- 15 K. Wang, S. Jinai, T. Urakami, H. Sato, M. Higashi, S. Tsujimura, Y. Kobori, R. Adachi, A. Yamakata and Y. Ie, *Angew. Chem., Int. Ed.*, 2024, **63**, e202412691.
- 16 D. Klintuch, K. Krekić, C. Bruhn, Z. Benkő and R. Pietschnig, *Eur. J. Inorg. Chem.*, 2016, 718–725.
- 17 F. Roesler, M. Kovács, C. Bruhn, Z. Kelemen and R. Pietschnig, *Organometallics*, 2023, **42**, 793–802.
- 18 G. Märkl and R. Potthast, *Angew. Chem., Int. Ed. Engl.*, 1967, **6**, 86.
- 19 J. Silberzahn, H. Pritzkow and H. P. Latscha, *Z. Naturforsch. B*, 1991, **46**, 197–201.
- 20 A. Fukazawa, Y. Ichihashi, Y. Kosaka and S. Yamaguchi, *Chem. – Asian J.*, 2009, **4**, 1729–1740.
- 21 C. Wang, A. Fukazawa, M. Taki, Y. Sato, T. Higashiyama and S. Yamaguchi, *Angew. Chem., Int. Ed.*, 2015, **54**, 15213–15217.
- 22 R. A. Adler, C. Wang, A. Fukazawa and S. Yamaguchi, *Inorg. Chem.*, 2017, **56**, 8718–8725.
- 23 C. Wang, M. Taki, Y. Sato, A. Fukazawa, T. Higashiyama and S. Yamaguchi, *J. Am. Chem. Soc.*, 2017, **139**, 10374–10381.
- 24 N. Burford, R. E. V. H. Spence, A. Linden and T. S. Cameron, *Acta Crystallogr., Sect. C: Cryst. Struct. Commun.*, 1990, **46**, 92–95.
- 25 V. M.-Y. Leung, H.-C. F. Wong, C.-M. Pook, Y.-L. S. Tse and Y.-Y. Yeung, *Chem. Sci.*, 2023, **14**, 12684–12692.
- 26 F. H. Allen, O. Kennard, D. G. Watson, L. Brammer, A. G. Orpen and R. Taylor, *J. Chem. Soc., Perkin Trans. 2*, 1987, S1–S19.
- 27 K. Kveseth, R. Seip and D. A. Kohl, *Acta Chem. Scand.*, 1980, **34a**, 31–42.
- 28 E. Kryachko and S. Scheiner, *J. Phys. Chem. A*, 2004, **108**, 2527–2535.
- 29 M. E. Squillacote, R. S. Sheridan, O. L. Chapman and F. A. L. Anet, *J. Am. Chem. Soc.*, 1979, **101**, 3657–3659.
- 30 M. K. Bera, C. Chakraborty and S. Malik, *J. Mater. Chem. C*, 2017, **5**, 6872–6879.
- 31 Y. Zhang, H. Mao, W. Xu, J. Shi, Z. Cai, B. Tong and Y. Dong, *Chem. Eur. J.*, 2018, **24**, 15965–15977.
- 32 M. K. Bera, P. Pal and S. Malik, *J. Mater. Chem. C*, 2020, **8**, 788–802.
- 33 P. Pal, A. Datta, S. Mukherjee, A. Perumal and S. Malik, *J. Mater. Chem. C*, 2023, **11**, 16594–16604.
- 34 P. Pal, A. Datta, R. Mondal and S. Malik, *ACS Appl. Polym. Mater.*, 2024, **6**, 6001–6009.

